# Structures and lifetimes of states in $^{110}$Cd

F. Corminboeuf,[1,*] T. B. Brown,[2] L. Genilloud,[1] C. D. Hannant,[2] J. Jolie,[1] J. Kern,[1,†] N. Warr,[2] and S. W. Yates[2]
[1]*Institut de Physique, Université de Fribourg, Pérolles, CH-1700 Fribourg, Switzerland*
[2]*University of Kentucky, Lexington, Kentucky 40506-0055*
(Received 14 April 2000; published 8 December 2000)

A set of measurements consisting of $\gamma$-ray excitation functions and angular distributions has been performed using the $(n,n'\gamma)$ reaction on $^{110}$Cd. Gamma-ray excitation functions allowed us to clarify the level scheme by placing ten new transitions and to establish one new level. From $\gamma$-ray angular distributions, the lifetimes for 16 excited states were extracted using the Doppler-shift attenuation method. The experimental $B(E2)$, $B(M1)$, and $B(E1)$ values of transitions from intruder, octupole, and three-phonon states are compared to different theoretical models.

DOI: 10.1103/PhysRevC.63.014305 PACS number(s): 21.10.Tg, 23.20.Js, 25.40.Fq, 27.60.+j

## I. INTRODUCTION

The $Z=50$ mass region is very favorable for nuclear structure studies due to the large abundance of stable isotopes combined with the interesting feature of neutrons at midshell and protons near the $Z=50$ shell closure. In this region, $^{110}$Cd emerged early as a classic example of a vibrational nucleus [1,2]. However, although the excited nucleus showed the two-phonon states expected for a vibrator, additional levels were observed forming a deformed band up to $J^{\pi}=6^{+}$ [3]. These states were interpreted as evidence of shape coexistence, where two-particle–two-hole (2*p*-2*h*) excitations across the $Z=50$ closed proton shell drive the nucleus into deformation [4]. Both types of excitations have been studied up to higher spin by Kern *et al.* [5].

Numerous experiments have been performed to develop the $^{110}$Cd level scheme, utilizing a wide variety of techniques, including transfer reactions [6,7], inelastic proton scattering [8,9], beta-decay measurements [9–12], inelastic neutron scattering [13,14], and the $(\alpha,2n)$ reaction [5,9]. An extensive level scheme has been developed, including lifetimes for the excited states with high spins [15,16]. Some years ago, the nature of low-spin states was studied state by state through in-beam techniques and many multiphonon states were proposed [12]. However, because of the absence of measured lifetimes, complete characterization of these states was not possible.

With the aim of extending the knowledge of lifetimes of low-spin states, measurements at the University of Kentucky Van de Graaff facility have been performed using the Doppler-shift attenuation method (DSAM) following inelastic neutron scattering. The experiments consisted of $\gamma$-ray excitation functions and angular distributions. The former allowed us to extend the level scheme by ten new transitions and add one new level. The latter yielded lifetimes of 16 excited states in $^{110}$Cd, in particular for the three-phonon, intruder, and octupole states. In addition, multipole mixing ratios were measured. The complete data set is compared with different theoretical descriptions incorporating shape coexistence. A portion of these results has been presented in Ref. [17] in the context of the collectivity of the three-phonon states.

*Electronic address: frederic.corminboeuf@unifr.ch
†Deceased.

## II. EXPERIMENTAL RESULTS

Gamma rays were observed following the $^{110}$Cd$(n,n'\gamma)$ reaction with the facilities at the University of Kentucky accelerator laboratory [18]. For the excitation function measurements, $\gamma$-ray spectra were recorded in 0.1-MeV increments of incident neutron energy, and angular distribution measurements were performed at two neutron energies. The approximately monoenergetic neutrons ($\Delta E_n \sim 100$ keV) for these measurements were produced with the $^3$H$(p,n)$ reaction. Protons from the University of Kentucky Van de Graaff accelerator were pulsed at a 1.875 MHz rate with a pulse width of $<2$ ns. The pulsed proton beam with an average current of 1.8 $\mu$A was focused through an 8 $\mu$m molybdenum entrance foil into a 1 cm$\times$3 cm tantalum-lined stainless steel gas cell containing approximately 1 atm of tritium gas. The scattering sample consisted of three ingots of cadmium metal, enriched to 97.25% in $^{110}$Cd, arranged in a nearly cylindrical geometry with a diameter of 1.2 cm and a height of 2.4 cm. This scattering sample was suspended 3.0 cm from the end of the gas cell.

### A. $\gamma$-ray excitation functions

A $\gamma$-ray excitation function measurement was performed with the aim of clarifying the decay scheme of low-spin states. It consisted of varying the energy of the incident neutrons from 2.1 to 3.4 MeV in 0.1-MeV steps. The experiment was performed using a $\sim$50% (relative) efficient HPGe detector located 125 cm from the scattering sample. The detector was placed inside a BGO anti-Compton shield and had an energy resolution of 2.0 keV at 1.33 MeV. Time-of-flight gating was used to reduce extraneous background events. Figure 1 shows the $\gamma$-ray spectrum acquired at $E_n=3.4$ MeV. Figure 2 shows excitations functions for selected $\gamma$ rays. In all cases the branching ratios of the used transitions were considered in order to extract the experimental excitation function yields. The theoretical excitation functions were calculated with the program CINDY [19], and the

 

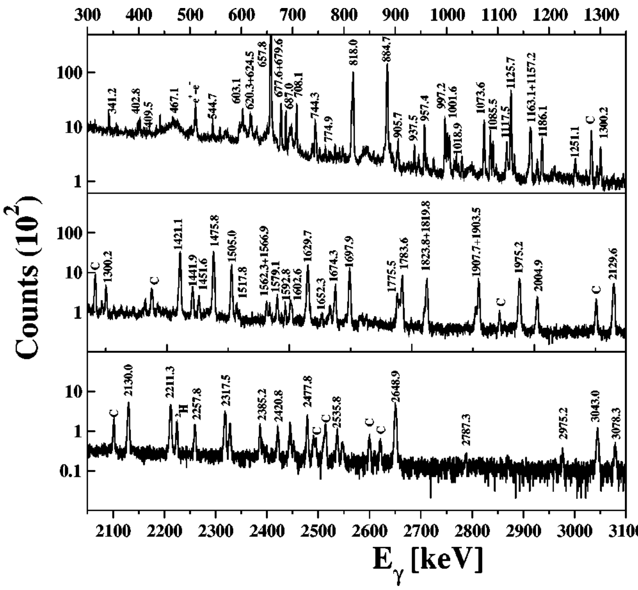


FIG. 1. Gamma-ray spectrum acquired at $E_n=3.4$ MeV. The prominent peaks from $^{110}$Cd are labeled with their energies in keV. Peaks marked with C are contaminants.

data were normalized to the calculated values using levels with known spins. The relative shapes of the excitation functions also proved helpful in assessing the possible spin values; however, it is not possible to determine the parities of the states. Therefore, we adopt, in general, the same parities as given in Ref. [20].

### B. $\gamma$-ray angular distribution

Gamma-ray angular distributions measurements were performed at neutron energies of 3.2 and 2.9 MeV. The latter energy was chosen to avoid the population of higher-lying levels which could feed the states of interest and perturb the measured lifetimes and to maximize the population of the levels of interest.

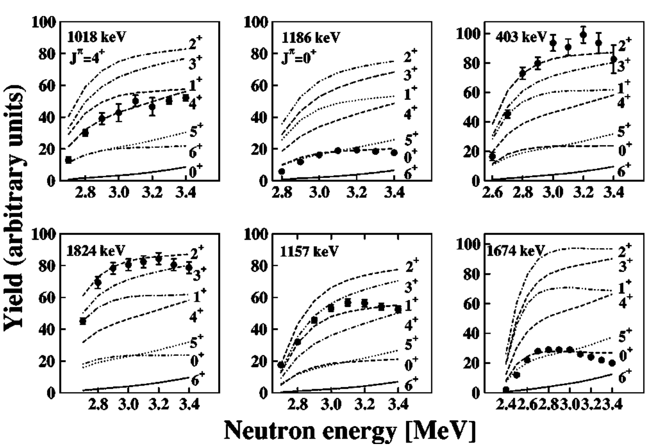


FIG. 2. Excitation functions for $\gamma$ rays from levels with known spins [$4^+$ (2561), $0^+$ (2662)], the 403-keV and 1824-keV $\gamma$ rays from the 2482-keV level, the 1157-keV $\gamma$ rays from the 2633-keV level, and the 1674-keV $\gamma$ rays from the 2332-keV level compared with calculations from the program CINDY [19].

The Doppler-shift attenuation measurement consisted of determining the energy of a $\gamma$ ray emitted at various angles. The energy of the observed $\gamma$ ray, $E_\gamma$, at an angle $\theta_\gamma$ with respect to the recoil direction is given by

$$E_\gamma(\theta)=E_0[1+\beta F(\tau)\cos\theta_\gamma], \tag{1}$$

where $E_0$ is the unshifted $\gamma$-ray energy and $\beta=v/c$, with $v$ the recoil velocity of the nucleus in the center-of-mass frame. The lifetimes of the states can be determined by comparison of the measured $F(\tau)$ values with those calculated using the Winterbon formalism [21]. A description of the method can be found in Ref. [22].

The 2.9-MeV measurement was performed with spectra recorded at 11 angles using the same detector placed inside a BGO anti-Compton shield and the same geometry as for the $\gamma$-ray excitation function measurement. The energy resolution was 2.2 keV at 1.33 MeV. The experiment at 3.2 MeV was performed with spectra recorded at seven angles using a $\sim$50% (relative) efficient HPGe detector located at 112.5 cm from the scattering sample. The 2.9-MeV measurement was used for the lower-lying states, in order to minimize the effects of feeding.

The energy calibration of the detectors was simultaneously monitored through the use of radioactive sources of $^{24}$Na, $^{60}$Co, and $^{133}$Ba during the acquisition of the in-beam spectra. Because $\gamma$ rays from the $(n,n'\gamma)$ reaction and those from the radioactive sources are recorded simultaneously, reliable Doppler shifts can be measured even when these shifts are quite small, i.e., 0.1 keV. In fact, the energy shifts of the in-beam $\gamma$ rays relative to the internal calibration lines or to other $\gamma$ rays from long-lived ($>$2 ps) states largely determine the precision with which lifetimes can be measured. In order to take into account all transitions depopulating a level, we have combined the results from these transitions to obtain a weighted average value of $F(\tau)$ for each level. Examples of levels with lifetimes too long to be determined by DSAM are presented in Fig. 3. In Figs. 4 and 5, the $\gamma$-ray energies, measured at $E_n=2.9$ MeV, are plotted as a function of angle for the most intense transitions from levels of interest. In order to test the lifetimes obtained, we have compared our values with previously published results from Refs. [15,16]. As Table I shows, the results are in agreement with the literature values. Because of the large uncertainty of the lifetime for the three-phonon $6^+$ state in our measurement, the value from Ref. [16] was adopted which, while in agreement with our value, is more precise (see Table I).

The $\gamma$-ray angular distributions performed at $E_n=2.9$ MeV were fitted with a Legendre polynomial expansion, allowing us to extract multipole-mixing ratios for the $\gamma$-ray transitions from the levels of interest. When two $\delta$ values were possible, the one in better agreement with the tabulated values in Refs. [5,20] was chosen. In Table II the experimental values are compared with those from previous measurements [5,20]. Figure 6 presents results of the angular distribution analysis for a few transitions of $^{110}$Cd.

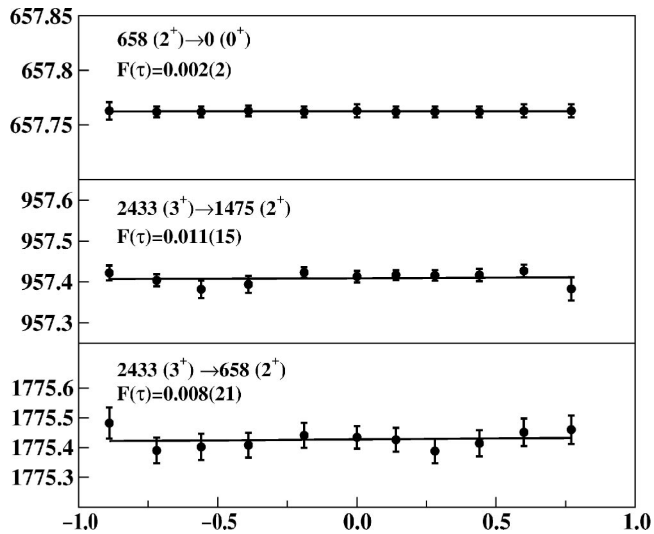


FIG. 3. Measured $\gamma$-ray energies as a function of cos $\theta$ for transitions with lifetimes too long to be determined with the DSAM.

## III. LEVEL SCHEME

In this section, we discuss levels which were expected to be observed but were not, those for which the decay is revised, and a new level. Transitions were placed on the basis of the excitation function thresholds and from $\gamma$-ray energy arguments. The experimental results are summarized in Table III. Some levels observed in transfer reactions have no known decay; from our data these levels cannot be confirmed and they must be regarded as doubtful. We placed 77 of the 128 $\gamma$ rays assigned to $^{110}$Cd in the measurement performed at $E_n = 3.4$ MeV during the $\gamma$-ray excitation function. The energy calibrations of the spectra were performed using the well-known energies of the radioactive sources of $^{60}$Co, $^{24}$Na, and with 11 well-known $\gamma$ rays in $^{110}$Cd taken from Ref. [5].

*1783.5-keV level.* This level was known to decay by transitions of 1125.7 and 1783.6 keV. An additional 310-keV transition depopulating this level was observed by Meyer and Peker [3] in their study of $^{110}$Cd from $\beta$ decay and by Araddad *et al.* [13] in their study of $^{110}$Cd with the $(n,n'\gamma)$ reaction. This $\gamma$ ray was also observed in our study and, on the basis of its excitation function threshold, it was also placed as depopulating the 1783.6-keV level. In contrast to earlier work, its relative intensity was determined.

*1809.5-keV level.* This level was first observed by Sarantites *et al.* [23] who proposed $J^\pi = (1,2)^+$ based on $^{110m}$In

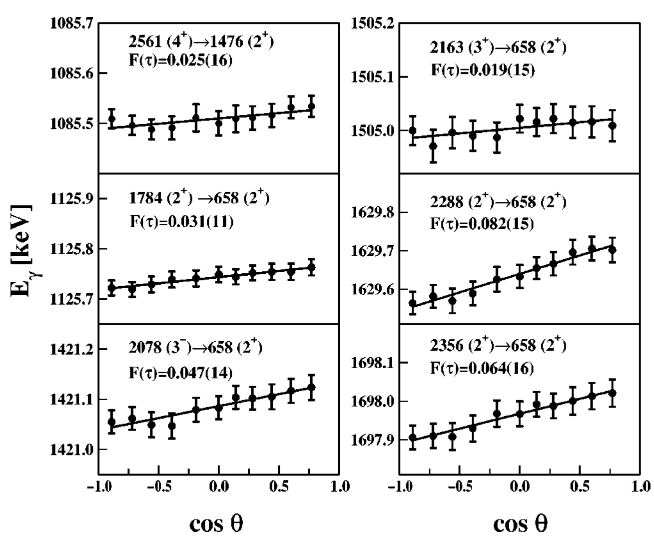


FIG. 4. Measured $\gamma$-ray energies as a function of cos $\theta$ for transitions from several levels of interest. $F(\tau)$ values are indicated.

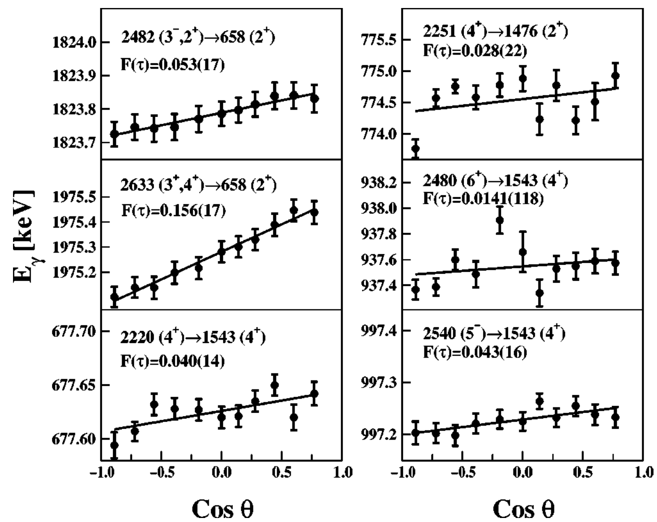


FIG. 5. Same caption as Fig. 4, but for additional $\gamma$ rays.

TABLE I. Measured lifetimes and comparisons with values from previous work [16,20].

| | | $\tau$ [ps] | |
|---|---|---|---|
| $E_x$ [keV] | $J^\pi_{adopted}$ | Literature | Present |
| 1783.5 | $2^+_{1,intr}$ | $1.44^{+2.00}_{-0.60}$ | $1.16^{+0.49a}_{-0.27}$ |
| 2078.8 | $3^-_{oct}$ | $1.05^{+0.50}_{-0.35}$ | $0.67^{+0.21a}_{-0.13}$ |
| 2162.8 | $3^+_{3ph}$ | | $1.20^{+0.83a}_{-0.35}$ |
| 2220.1 | $4^+_{3ph}$ | | $0.97^{+0.43a}_{-0.23}$ |
| 2250.6 | $4^+_{intr}$ | | $0.87^{+0.71a}_{-0.28}$ |
| 2287.4 | $2^+_{2,intr}$ | | $0.42^{+0.10a}_{-0.07}$ |
| 2355.7 | $2^+_{3ph}$ | | $0.51^{+0.17a}_{-0.10}$ |
| 2480.0 | $6^+_{3ph}$ | $0.58^{+0.22}_{-0.13}$ | $0.23^{+1.11a}_{-0.12}$ |
| 2481.6 | $(2^+)$ | | $0.67^{+0.33a}_{-0.17}$ |
| 2539.7 | $5^-_{oct}$ | $0.90^{+0.40}_{-0.25}$ | $0.83^{+0.51a}_{-0.23}$ |
| 2561.3 | $4^+$ | | $1.25^{+1.20a}_{-0.42}$ |
| 2633.1 | $(2^+, 3^+)$ | | $0.20^{+0.03a}_{-0.02}$ |
| 2649.5 | $(1^-)$ | | 0.04(1)[b] |
| 2758.2 | $(2^+,3^+)$ | | $0.33^{+0.13a}_{-0.08}$ |
| 2787.4 | $(2^+)$ | | 0.04(1) [b] |
| 2984.5 | $5^-$ | | $0.16^{+0.29b}_{-0.07}$ |

[a]From the $\gamma$-ray angular distribution performed at $E_n = 2.9$ MeV.
[b]From the $\gamma$-ray angular distribution performed at $E_n = 3.2$ MeV.

TABLE II. Comparison of measured multipole mixing ratios with previous work.

| $E_{level}$ [keV] | $J_i^\pi$ | $J_f^\pi$ | $E_\gamma$ [keV] | $\delta_{(n,n'\gamma)}$ | From Ref. [5] | From Ref. [20] |
|---|---|---|---|---|---|---|
| 1783.5 | $2^+_{1,intr}$ | $0^+$ | 310.5 | [a] | | |
| | | $2^+$ | 1125.7 | $0.13^{+0.03}_{-0.02}, 1.69^{+0.13}_{-0.11}$ | | 0.33(8) |
| | | $0^+$ | 1783.6 | $E2$ | | $E2$ |
| 2078.8 | $3^-_{oct}$ | $2^+$ | 603.1 | 0.04(2) | -0.14(22) | [b] |
| | | $2^+$ | 1421.1 | $0.003^{+0.028}_{-0.019}$ | 0.01(8) | 0.05(5) |
| 2162.8 | $3^+_{3ph}$ | $4^+$ | 620.3 | $-0.46^{+0.07}_{-0.06}, -1.61^{+0.21}_{-0.19}$ | | -0.70(4) |
| | | $2^+$ | 687.0 | $-1.66^{+0.09}_{-0.06}$ | -1.26(41) | -1.76(6) or -1.48(15) |
| | | $2^+$ | 1505.0 | $-1.52^{+0.11}_{-0.14}, -0.39^{+0.04}_{-0.05}$ | -1.48(23) | -1.21(4) |
| 2220.1 | $4^+_{3ph}$ | $4^+$ | 677.6 | -0.41(2) | -0.40(7) | -0.36(3) |
| | | $2^+$ | 744.3 | $E2$ | | 0(+16,-10) |
| | | $2^+$ | 1562.3 | $E2$ | $E2$ | -0.10(+2,-3) |
| 2250.6 | $4^+_{intr}$ | $2^+$ | 467.1 | $E2$ | $E2$ | $(E2)$ |
| | | $4^+$ | 708.1 | $0.13^{+0.04}_{-0.03}$ | -0.72(32) | -0.15(9) |
| | | $2^+$ | 774.9 | $E2$ | $E2$ | $(E2)$ |
| | | $2^+$ | 1592.8 | $E2$ | $E2$ | $(E2)$ |
| 2287.4 | $2^+_{2,intr}$ | $2^+$ | 1629.7 | $2.39^{+0.13}_{-0.18}$,-0.01(2) | | 0.06(3) |
| 2355.7 | $2^+_{3ph}$ | $0^+$ | 624.5 | $E2$ | | |
| | | $2^+$ | 1697.9 | -0.07(2),$2.86^{+0.21}_{-0.22}$ | | 0.10(5) or 1.8(5) |
| 2480.0 | $6^+_{3ph}$ | $4^+$ | 937.5 | $E2$ | $E2$ | $E2$ |
| 2481.6 | $(2^+)$ | $2^+$ | 1823.8 | $-0.91^{+0.09}_{-0.12}$,-2.88(56) | | -0.70(10) or -5.2(20) |
| | | $3^-$ | 402.8 | $E1$ | | |
| 2539.7 | $5^-_{oct}$ | $3^-$ | 460.8 | $(E2)$ | $E2$ | $(E2)$ |
| | | $4^+$ | 997.2 | $E1$ | -0.030(46) | -0.025(+35,-75) |
| 2561.3 | $4^+$ | $4^+$ | 1018.9 | $-0.49^{+0.16}_{-0.19}, 3.48^{+2.25}_{-1.23}$ | -0.56(35) | [b] |
| | | $2^+$ | 1085.5 | $E2$ | $E2$ | $E2$ |
| | | $2^+$ | 1903.5 | $E2$ | | |
| 2705.6 | $4^+_{intr}$ | $4^+$ | 1163.1 | $E2$ | 0.0(3) | |

[a]No reliable value was found.
[b]Same value as in Ref. [5].

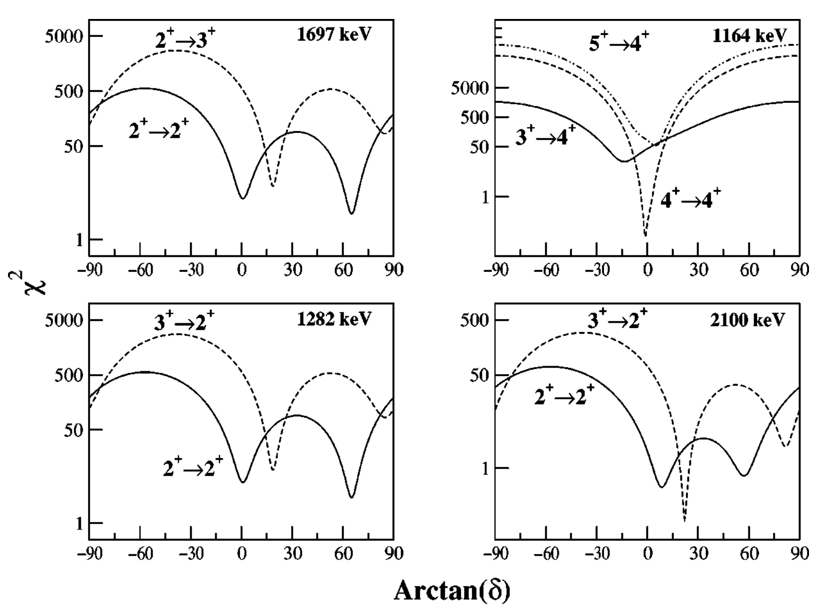


FIG. 6. Analysis of the angular distribution performed at 2.9 MeV of a few transitions in $^{110}$Cd. Shown is the $\chi^2$ calculated as a function of arctan($\delta$).

TABLE III. Observed transitions and levels.

| $E_x$ [keV][a] | $J^{\pi}_{adopted}$ | $J^{\pi}_{f}$ | $E_{\gamma}$ [keV] | $\delta$ | Mult. | B.R.[b] | $J^{\pi}_{prev}$ |
|---|---|---|---|---|---|---|---|
| 0.0 | $0^+$ | | | | | | $0^+$ |
| 657.765(9) | $2^+$ | $0^+$ | 657.765(9) | | $E2$ | 1.000 | $2^+$ |
| 1473.053(30) | $0^+$ | $2^+$ | 815.31(3) | | | 1.000 | $0^+$ |
| 1475.785(19) | $2^+$ | $2^+$ | 818.03(4) | $1.49^{+0.28}_{-0.40}$ | $M1+E2$ | 0.624(4) | $2^+$ |
| | | $0^+$ | 1475.75(4) | | $E2$ | 0.376(4) | |
| 1542.467(25) | $4^+$ | $2^+$ | 884.68(4) | | $E2$ | 1.000 | $4^+$ |
| 1731.284(32) | $0^+$ | $2^+$ | 255.55(5) | | | 0.088(3) | $0^+$ |
| | | $2^+$ | 1073.62(7) | | | 0.912(3) | |
| 1783.529(32) | $2^+$ | $0^+$ | 310.53(12) | | $E2$ | 0.003(1) | $2^+$ |
| | | $2^+$ | 1125.71(2) | $0.13^{+0.03}_{-0.02}$ | $M1+E2$ | 0.756(2) | |
| | | $0^+$ | 1783.62(7) | | $E2$ | 0.240(2) | |
| 2078.853(30) | $3^-$ | $2^+$ | 295.62(9) | | | 0.032(6) | $3^-$ |
| | | $2^+$ | 603.10(4) | | $E1$ | 0.127(3) | |
| | | $2^+$ | 1421.08(4) | | $E1$ | 0.841(3) | |
| 2078.878(30) | $0^+$ | $2^+$ | 295.62(9) | | | 0.758(4) | $0^+$ |
| | | $2^+$ | 1421.08(4) | | | 0.242(4) | |
| 2162.798(26) | $3^+$ | $4^+$ | 620.33(4) | $-0.46^{+0.07}_{-0.06}$ | $M1+E2$ | 0.165(5) | $3^+$ |
| | | $2^+$ | 687.02(4) | $-1.66^{+0.09}_{-0.08}$ | $M1+E2$ | 0.247(7) | |
| | | $2^+$ | 1505.03(4) | $-1.52^{+0.11}_{-0.14}$ | $M1+E2$ | 0.587(9) | |
| 2220.083(31) | $4^+$ | $4^+$ | 677.62(4) | -0.41(2) | $M1+E2$ | 0.638(8) | $4^+$ |
| | | $2^+$ | 744.29(4) | | $E2$ | 0.281(7) | |
| | | $2^+$ | 1562.33(8) | | $E2$ | 0.081(3) | |
| 2250.564(35) | $4^+$ | $2^+$ | 467.08(6) | | $E2$ | 0.081(4) | $4^+$ |
| | | $4^+$ | 708.10(4) | $0.13^{+0.04}_{-0.03}$ | $M1+E2$ | 0.817(6) | |
| | | $2^+$ | 774.88(20) | | $E2$ | 0.033(4) | |
| | | $2^+$ | 1592.79(10) | | $E2$ | 0.069(4) | |
| 2287.425(61) | $2^+$ | $2^+$ | 1629.66(55) | -0.01(2) | | 1.000 | $2^+$ |
| 2332.045(71) | $0^+$ | $2^+$ | 1674.28(7) | | | 1.000 | $(0^+,1^+,2^+)$ |
| 2355.717(57) | $2^+$ | $0^+$ | 624.47(9) | | $E2$ | 0.030(2) | $2^+$ |
| | | $2^+$ | 1697.93(7) | -0.07(2) | $M1+E2$ | 0.970(2) | |
| 2433.206(33) | $3^+$ | $2^+$ | 957.41(4) | | | 0.641(7) | $3^+$ |
| | | $2^+$ | 1775.48(5) | | | 0.359(7) | |
| 2477.544(98) | $2^+$ | $0^+$ | 746.19(17) | | $E2$ | 0.164(7) | $1^+,2^+$ |
| | | $2^+$ | 1001.65(17) | | $(E2)$ | 0.394(6) | |
| | | $2^+$ | 1819.82(24) | | | 0.080(4) | |
| | | $0^+$ | 2477.81(22) | | $E2$ | 0.360(7) | |
| 2480.019(74) | $6^+$ | $4^+$ | 937.55(7) | | $E2$ | 1.000 | $6^+$ |
| 2481.644(121) | $(2^+)$ | $3^-$ | 402.84(17) | | $E1$ | 0.119(12) | $3^-,2^+$ [c] |
| | | $2^+$ | 1823.83(17) | $-0.91^{+0.09}_{-0.12}$ | $M1+E2$ | 0.881(12) | |
| 2539.690(47) | $5^-$ | $3^-$ | 460.83(17) | | $(E2)$ | 0.030(4) | $5^-$ |
| | | $4^+$ | 997.22(4) | | $E1$ | 0.970(4) | |
| 2561.278(39) | $4^+$ | $4^+$ | 1018.86(8) | $-0.49^{+0.16}_{-0.19}$ | $M1+E2$ | 0.136(6) | $4^+$ |
| | | $2^+$ | 1085.49(5) | | $E2$ | 0.683(8) | |
| | | $2^+$ | 1903.48(7) | | $E2$ | 0.182(7) | |
| 2633.070(121) | $(2^+,3^+)$ | $2^+$ | 1157.24(17) | | | 0.030(4) | $2^+$ [d]$,(3^+),4^+$ [c] |
| | | $2^+$ | 1975.35(17) | | $(E2)$ | 0.970(4) | |
| 2649.537(108) | $(1^-)$ | $0^+$ | 1176.60(8) | | | 0.094(4) | $(0^-,1^-)$ |
| | | $0^+$ | 2649.39(9) | | | 0.906(4) | |
| 2659.955(60) | $5^-$ | $4^+$ | 409.51(14) | | | 0.078(10) | $5^-$ |
| | | $4^+$ | 1117.46(6) | | | 0.922(10) | |
| 2661.988(74) | $0^+$ | $2^+$ | 1186.13(5) | | | 0.535(7) | $0^+$ |
| | | $2^+$ | 2004.33(6) | | | 0.465(7) | |
| 2705.589(65) | $4^+$ | $4^+$ | 1163.12(6) | | $E2$ | 1.000 | $4^{(-)}$ |

TABLE III. *(Continued).*

| $E_x$ [keV][a] | $J^{\pi}_{adopted}$ | $J^{\pi}_{f}$ | $E_{\gamma}$ [keV] | $\delta$ | Mult. | B.R.[b] | $J^{\pi}_{prev}$ |
|---|---|---|---|---|---|---|---|
| 2707.443(51) | $4^+$ | $3^+$ | 544.67(6) | | $(M1+E2)$ | 0.307(9) | $(4^+)$ |
| | | $4^+$ | 1164.94(7) | | $(M1)$ | 0.693(9) | |
| 2758.173(71) | $(2^+,3^+)$ | $2^+$ | 1282.28(7) | | | 0.725(6) | $(1^+,2^+,3^+)$ |
| | | $2^+$ | 2100.57(9) | | | 0.275(6) | |
| 2787.375(71) | $(2^+)$ | $2^+$ | 2129.61(7) | | $M1+E2$ | 1.000 | $1^+,2^+$ |
| 2793.400(56) | $(4^+)$ | $4^+$ | 573.23(9) | | | 0.311(15) | $(4^+)$ |
| | | $3^+$ | 630.59(9) | | | 0.336(17) | |
| | | $4^+$ | 1251.02(9) | | | 0.353(19) | |
| 2842.688(64) | $5^-$ | $5^-$ | 182.83(60)[e] | | | | $(5^-)$ |
| | | $3^+$ | 409.51(14) | | | 0.081(27) | |
| | | $4^+$ | 1300.21(7) | | $(E1)$ | 0.922(27) | |
| 2868.998(43) | $(2^+)$ | $2^+$ | 1085.49(5) | | $E2$ | 0.354(5) | $1^+,2^+$ |
| | | $2^+$ | 2211.27(7) | | | 0.646(5) | |
| 2917.590(61) | $2^+,3^-$ | $4^+$ | 356.40(10) | | | 0.120(14) | $2^+,3^-$ |
| | | $2^+$ | 1441.85(12) | | | 0.480(33) | |
| | | $2^+$ | 2259.73(9) | | | 0.400(26) | |
| 2926.723(79) | $5^+$ | $3^+$ | 763.95(9) | | | 0.576(26) | $5^+$ |
| | | $4^+$ | 1384.19(14) | | | 0.424(26) | |
| 2975.164(90) | $2^+$ | $2^+$ | 2317.40(9) | | | 1.000 | $2^+$ |
| 2984.501(94) | $5^-$ | $3^-$ | 905.71(7) | | | 0.445(21) | $5^-$ |
| | | $4^+$ | 1441.85(12) | | | 0.555(21) | |
| 2993.615(171) | $(0^+)$[f] | $2^+$ | 1517.83(17) | | | 1.000 | $0^+,3^+,4^+$ [d] |
| 2994.089(84) | $(3^+,4^+)$[f] | $4^+$ | 1451.62(8) | | | 1.000 | $0^+,3^+,4^+$ [d] |
| 3042.841(83) | $(2^+)$ | $2^+$ | 1566.92(10) | | | 0.158(8) | |
| | | $2^+$ | 2385.22(11) | | | 0.352(10) | |
| | | $0^+$ | 3042.98(28) | | | 0.491(10) | |

[a]Energy calculated using a least-squares procedure involving all transitions placed in the present level scheme.
[b]From this experiment.
[c]From Ref. [13].
[d]From Ref. [7].
[e]This transition was not observed in our experiments due to the attenuation of low-energy $\gamma$ rays in the sample. We have accepted the value given in Ref. [5].
[f]See discussion in the text.

decay. From their study of the same decay, Bertschy *et al.* [12] noted this level as questionable. Such a low-spin state should be populated by the $(n,n')$ reaction, but no evidence for its existence was observed in this study. We conclude that this earlier level placement is spurious.

*2078.86- and 2078.88-keV levels.* This doublet is well established. The main difficulty lies in separating the $\gamma$ rays which decay from each of these states. We observe $\gamma$ rays with energies of 295.6, 603.1, and 1421.1 keV. Taking into account the branching ratio given in Ref. [20], the measured intensities for these transitions agree with the proposed $0^+$, $3^-$ doublet.

*2332.0-keV level.* This level was assigned by Blasi *et al.* [7] from $(\vec{d},t)$ reaction measurements as $J^{\pi}=0^+$, while according to Ref. [20] it has $J^{\pi}=(0^+,1^+,2^+)$. The excitation function supports $J^{\pi}=(0^+,1^+)$ (see Fig. 2), and the angular distribution of the $\gamma$ ray from this level is isotropic. Consequently, we assign this level as $J^{\pi}=0^+$.

*2355.7-keV level.* The $\gamma$-ray excitation function measurement allowed us to improve our knowledge of the decay of this three-phonon state $(2^+_{3ph})$ to the two-phonon multiplet, because a transition of 624.5 keV from this state to the $0^+$ state at 1731 keV is observed [17].

*2477.5-keV level.* This level was observed by Blasi *et al.* [7] and Bertschy *et al.* [12]. Based on its excitation function, the 2477.8-keV transition, which decays to the ground state, was also placed as in Ref. [12]. Moreover, the level decays by additional transitions of 1819.8 keV $[2477.5 \rightarrow 657.7(2^+_{1ph})]$ and 746.2 keV $[2477.5 \rightarrow 1731.3(0^+_{2ph})]$. From the $E2$ multipolarity of the latter transition, we assign this level as $J^{\pi}=2^+$ in agreement with Ref. [7]. Bertschy *et al.* [12] observed a 1001-keV transition from this level, but this transition is placed in Ref. [20] as depopulating the 3078-keV level. The lower placement is supported by the $\gamma$-ray excitation function of this transition for which the observed threshold is about 2500 keV. Therefore, this transition was retained as depopulating the 2477-keV level.

*2481.6-keV level.* This level is known to be depopulated by a transition of 1823.9 keV to the 657.7-keV level $(2^+_{1ph})$. From the excitation function data, a 402.8-keV transition is found which connects this level to the 2078.9-keV level $(3^-_{oct})$. This state was assigned by Araddad *et al.* [13] as $J^\pi=3^-,2^+$. As shown in Fig. 2, the excitation function favors a spin $J=(2)$. Moreover, the multipolarities of the decaying transitions indicate positive parity. Consequently, we adopt the assignment $J^\pi=(2^+)$ for this level.

*2633.1-keV level.* A new transition of 1157.2 keV $[2633.1\rightarrow 1475.8(2^+_{2ph})]$ from this level is observed. Araddad *et al.* [13] proposed $J^\pi=(3^+),4^+$, Blasi *et al.* [7] assigned $J^\pi=2^+$, and Bertschy *et al.* [12] proposed $J^\pi=2^+,(3^+)$. The excitation function of the 1975.4-keV transition, which was known to deexcite this level, supports a spin and parity of $J^\pi=(3^+)$. Combining all these data, we adopt $J^\pi=(2^+,3^+)$

*2649.5-keV level.* The level energy has been improved from 2649.15(24) keV (from Ref. [20]) to 2649.54(11) keV. This state was assigned according to Ref. [20] as $J^\pi=(0^-,1^-)$. Moreover, it decays only to $0^+$ states and the excitation function favors a spin of $J=1$. We adopt the spin and parity of $J^\pi=(1^-)$ for this level.

*2707.4-keV level.* This level was assigned by Kern *et al.* [5] in their study of the $^{108}$Pd$(\alpha,2n)^{110}$Cd reaction and Blasi *et al.* [7] as $J^\pi=4^+$, but this assignment is listed as uncertain in Ref. [20]. The excitation function data also support a spin of 4 for this level. As shown in Fig. 6, the angular distribution analysis of the 1164-keV transition favors also a spin of 4. Therefore, we confirm $J^\pi=4^+$ for this level.

*2758.2-keV level.* This level is assigned in Ref. [20] as $J^\pi=1^+,2^+,3^+$. Araddad *et al.* [13] observed a spin and parity of $J^\pi=3^+$ and Blasi *et al.* [7] assigned this level as $J^\pi=1^+,2^+$. As one can see in Fig. 6, the angular distribution of the 1282-keV transition seems to favor $J^\pi=2^+$ while the 2100-keV transition favors $J^\pi=3^+$. The multipole mixing ratios of the transitions support positive parity, so we adopt for this level the assignment of $J^\pi=(2^+,3^+)$.

*2787.3-keV level.* This level was assigned by Bertschy *et al.* [12] and Blasi *et al.* [7] as $J^\pi=1^+,2^+$. The excitation function favors $J^\pi=(2^+)$ for this level.

*2842.7-keV level.* This level was known to decay by transitions of 182.8, 409.5, and 1300.2 keV. The spin and parity were proposed to be $J^\pi=5^-$ by Kern *et al.* [5], but it is listed as uncertain in Ref. [20]. From the excitation function data and the multipole character of the 1300-keV transition, we also assign this level as $J^\pi=5^-$.

*2869.0-keV level.* The spin of this level was assigned by Bertschy *et al.* [12] and Blasi *et al.* [7] as $J^\pi=2^+$, and according to Ref. [20] it has $J^\pi=1^+,2^+$. From the excitation function data, this level seems to have a spin and parity of $J^\pi=(2^+)$, which is the value we adopt.

*2984.5-keV level.* This level was observed by Kern *et al.* [5] to decay by only a 1441.8-keV transition. A new transition of 905.7 keV $[2984.5\rightarrow 2078.8(3^-_{oct})]$ has been placed. This $\gamma$ ray was also observed by Kern *et al.* [5], but was not placed in the level scheme. From the excitation function data, the spin and parity of $J^\pi=5^-$, assigned by Kern *et al.* [5] are supported.

*2994-keV doublet.* Blasi *et al.* [7] observed an unresolved doublet at this energy. New transitions of 1451.6 and 1517.8 keV from the decay of these levels have been added. As the 1451.6-keV transition decays to the state at 1542 keV with $J^\pi=4^+$, we can support the $J^\pi=(3^+,4^+)$ assignment proposed by Blasi *et al.* [7]. The corresponding excitation energy would be 2994.0 keV. The second transition has an energy of 1517.8 keV. This $\gamma$ ray is placed as a transition depopulating the second member of the doublet at an excitation energy of 2993.4 keV. According to Ref. [7], the second level has $J^\pi=(0^+)$.

*3042.8-keV level.* This new level decays by transitions of 1566.9, 2385.2, and 3043.0 keV, but no multipolarities could be extracted for these transitions from the present data. The $\gamma$-ray excitation functions of the lines seem to indicate a spin and parity of $J^\pi=(2^+)$, which is in agreement with the decay pattern of this new level.

## IV. COMPARISON WITH THEORY

We limit ourselves here to the states below 2.55 MeV. This limitation is due to uncertain spin assignments of higher-lying states and the clear noncollective decay of other states, e.g., the 2561-keV state.

### A. Positive-parity states

In Table IV, the experimental $B(E2)$ values for transitions depopulating the states of interest are compared with theoretical predictions. Only states for which the spin-parity assignments have been unambiguously determined are given. In Ref. [17], several theoretical predictions available in the literature were compared with our data for the decay of the three-phonon states. The influence of two-particle, four-hole intruder configurations, which leads to a second collective structure, is studied in the present work. In order to take account of the shape coexistence [24] in $^{110}$Cd, which manifests itself at an energy near 1.5 MeV [5], models incorporating this feature are considered. The U(5)-O(6) model of Lehmann and Jolie [25] describes the normal states interacting with the intruder states by mixing the U(5) dynamic symmetry for the normal states and the O(6) limit for the intruder states. This model is very simple and has a reduced set of parameters.

Before comparing the U(5)-O(6) model and the experimental data, one should consider two facts. In Ref. [25], few absolute transition rates involving intruder states were used in the fit, and these involved analytic expressions between states that were assumed to interact only via two-level mixing. In order to include all mixings, numerical calculations with the code OCTUPOLE [26] were performed. Using the parameters of the U(5)-O(6) model given in Ref. [25], the numerical results given in Table IV (fourth column) are obtained.

In order to improve this model, we consider the electric quadrupole transition operator given by

$$T^{(E2)}=e_2[\delta_{N,N'}T_{U5}+\delta_{N+2,N'}\epsilon_{rel}T_{O6}], \qquad (2)$$

with the operators

TABLE IV. Comparison of experimental and theoretical $B(E2)$ values for states in $^{110}$Cd.

| Transition | $E_\gamma$ [keV] | Expt. [W.u.] | Theory [W.u.] U(5)-O(6) Lehmann and Jolie [25] | Theory [W.u.] U(5)-O(6) This work | IBM-2 [28] |
|---|---|---|---|---|---|
| $2^+_{1,intr}\rightarrow 0^+_{intr}$ [a] | 310.5 | $23^{+27}_{-18}$ | 15 | 52 | 44 |
| $2^+_{1,intr}\rightarrow 2^+_{1ph}$ [a] | 1125.7 | $0.16^{+0.12}_{-0.09}$ | 0.23 | 0.23 | 0.005 |
| $2^+_{1,intr}\rightarrow 0^+_{1ph}$ [a] | 1783.5 | 0.30(10) | 0.08 | 0.06 | 0.34 |
| $3^+_{3ph}\rightarrow 4^+_{2ph}$ | 620.3 | $7^{+6}_{-4}$ | 16 | 17 | 15 |
| $3^+_{3ph}\rightarrow 2^+_{2ph}$ | 687.0 | $25^{+13}_{-11}$ | 39 | 43 | 43 |
| $3^+_{3ph}\rightarrow 2^+_{1ph}$ | 1505.0 | $1.1^{+0.6}_{-0.5}$ | 0.002 | 0.002 | 0.4 |
| $4^+_{3ph}\rightarrow 4^+_{2ph}$ | 677.6 | $17^{+8}_{-6}$ | 26 | 29 | 23 |
| $4^+_{3ph}\rightarrow 2^+_{2ph}$ | 744.3 | 33(11) | 29 | 32 | 32 |
| $4^+_{3ph}\rightarrow 2^+_{1ph}$ | 1562.3 | 0.23(8) | 0.002 | 0.002 | 0.100 |
| $4^+_{intr}\rightarrow 2^+_{intr.}$ | 467.1 | $109^{+62}_{-53}$ | 27 | 113 | 124 |
| $4^+_{intr}\rightarrow 4^+_{2ph}$ | 708.1 | $2^{+4}_{-1}$ | 2 | 2 | 1 |
| $4^+_{intr}\rightarrow 2^+_{2ph}$ | 774.9 | $3^{+3}_{-1}$ | 0.30 | 0.30 | 0.02 |
| $4^+_{intr}\rightarrow 2^+_{1ph}$ | 1592.8 | $0.20^{+0.27}_{-0.10}$ | 0.0003 | 0.05 | 0.22 |
| $2^+_{2,intr}\rightarrow 2^+_{1ph}$ [b] | 1629.7 | $<0.004$ | 0.62 | 0.06 | 0.005 |
| $2^+_{3ph}\rightarrow 0^+_{2ph}$ | 624.5 | 16(5) | 18 | 26 | 19 |
| $2^+_{3ph}\rightarrow 2^+_{1ph}$ | 1697.9 | $0.02^{+0.02}_{-0.01}$ | 0.02 | 0.02 | 0.08 |
| $6^+_{3ph}\rightarrow 4^+_{2ph}$ | 937.5 | $62^{+18}_{-17}$ | 56 | 61 | 59 |
| $5^-_{oct}\rightarrow 3^-_{oct}$ | 460.8 | $48^{+27}_{-22}$ | 32 | 32 | – |

[a]First $2^+$ intruder state at $E_x=1783.5$ MeV.
[b]Second $2^+$ intruder state at $E_x=2287.5$ MeV.

$$T_{U5}=e_2([s^\dagger\tilde{d}+d^\dagger s]^{(2)}_\mu+\chi[d^\dagger\tilde{d}]^{(2)}_\mu) \qquad (3)$$

and

$$T_{O6}=e_2([s^\dagger\tilde{d}+d^\dagger s]^{(2)}_\mu). \qquad (4)$$

In Eq. (2), $e_2$ is the effective charge and $N'$ is the number of bosons. Each operator is applied to the respective states in each configuration. The parameter $\epsilon_{rel}$ weights the O(6) operator relative to the U(5) transition operator. In Ref. [25], $e_2=0.11$ [$e$ b], $\chi=-2.7$, and $\epsilon_{rel}=0.48$ were obtained. In order to remove the discrepancy in the description of the transition probabilities between the intruder states, in particular for the $4^+_{intr}\rightarrow 2^+_{1,intr}$ transition, the calculation was improved by changing the $\epsilon_{rel}$ parameter from 0.48 to 1.0 in Eq. (2). As can be observed in the fifth column of Table IV, this parameter value yields better agreement with the experimental results. This value for $\epsilon_{rel}$ is also more in line with the results obtained for the other Cd isotopes [25].

A more sophisticated calculation can be performed using the IBM-2 approach. In this model, neutron and proton bosons are considered. This distinction allows one to discern the effects due to the proton 2$p$-4$h$ configurations in more detail. Notably, it predicts the energy of these states on a semimicroscopic basis (see Ref. [27]), but at the cost of a greatly increased parameter set. Using this IBM-2 approach, calculations were performed by Délèze *et al.* [28] for $^{110,112,114}$Cd nearly a decade ago. These calculations were extensively tested for $^{112}$Cd in Refs. [29,30] and proved to be reliable. They are compared to our data in the last column of Table IV. Once more, excellent agreement is obtained. If we examine the fourth and fifth columns of Table IV, we see that changing the $\epsilon_{rel}$ from 0.48 to 1.00 in the U(5)-O(6) model yields results that are very close to the IBM-2 results. This can be illustrated by the presence of coherent mixing of intruder and three-phonon states as described in [31]. If all transitions decaying from the $3^+_{3ph}$, $4^+_{3ph}$, and $6^+_{3ph}$ states to the $2^+$ and $4^+$ two-phonon states are summed for each state, the common O(5) symmetry imposes equal mixing amplitudes for these two- and three-phonon states and hence the same sum for each state. This is not the case for the $2^+_{3ph}$ state which has another O(5) quantum number. Inspection of Table IV shows that indeed the summed decay probabilities are nearly equal in the U(5)-O(6) model. In Table V these values are compared to those in the IBM-2 and the experimental sums. One notices that the IBM-2 values are very close to each other. Unfortunately, the experimental sums still have errors that are too large to permit a definite experimental confirmation about the observation of this coherent mixing.

For both models, the experimental and theoretical level energies are in good agreement, as is illustrated in Fig. 7, in

TABLE V. The sum of $B(E2;J^+_{3ph}\rightarrow J^+_{2ph})$ for the three-phonon states which mix coherently in the U(5)-O(6) model, is compared to the IBM-2 and experimental sums.

| $J^\pi$ | U(5)-O(6) | IBM-2 | Expt. |
|---|---|---|---|
| $3^+_{3ph}$ | 61 | 58 | 32(14) |
| $4^+_{3ph}$ | 61 | 55 | 50(14) |
| $6^+_{3ph}$ | 61 | 59 | 62(18) |

which level energies and $B(E2)$ values calculated using the U(5)-O(6) model are compared with the experimental results. More details concerning the description of the models and the Hamiltonians can be found in Ref. [32].

Table VI shows a comparison between the experimental and theoretical $B(M1)$ values for the transitions of Table IV with mixed multipole character. They are compared to the theoretical IBM-2 values from Ref. [28]. Note that all $M1$ transitions are strictly forbidden in the U(5)-O(6) model. We remark as for the $B(E2)$ values that there is good agreement between theory and experiment and that all observed transition probabilities are quite small. One can also now clearly exclude the mixed symmetry character of the third experimental $2^+$ state which in the original calculation of Ref. [28] was associated with the theoretical lowest mixed-symmetry state. Note that at that time there was an additional experimental $2^+$ state at 1809.5 keV, which was shown not to exist by Bertschy *et al.* [12]. Although the presence in the theory

TABLE VI. Comparison of experimental and theoretical $B(M1)$ values for states in $^{110}$Cd.

| Transition | $E_\gamma$ [keV] | $B(M1)_{expt.}$ [$\mu_n^2$] | Theory [$\mu_n^2$] |
|---|---|---|---|
| $2^+_{1,intr}\rightarrow 2^+_{1ph}$ | 1125.7 | 0.026(8) | 0.007 |
| $3^+_{3ph}\rightarrow 4^+_{2ph}$ | 620.3 | 0.027(11) | 0.021 |
| $3^+_{3ph}\rightarrow 2^+_{2ph}$ | 687.0 | 0.010(4) | 0.018 |
| $3^+_{3ph}\rightarrow 2^+_{1ph}$ | 1505.0 | 0.002(1) | 0.001 |
| $4^+_{3ph}\rightarrow 4^+_{2ph}$ | 677.6 | 0.103(32) | 0.003 |
| $4^+_{intr}\rightarrow 4^+_{2ph}$ | 708.1 | $0.148^{+73}_{-68}$ | 0.001 |
| $2^+_{2,intr}\rightarrow 2^+_{1ph}$ | 1629.7 | 0.031(6) | 0.007 |
| $2^+_{3ph}\rightarrow 2^+_{1ph}$ | 1697.9 | 0.022(5) | 0.021 |

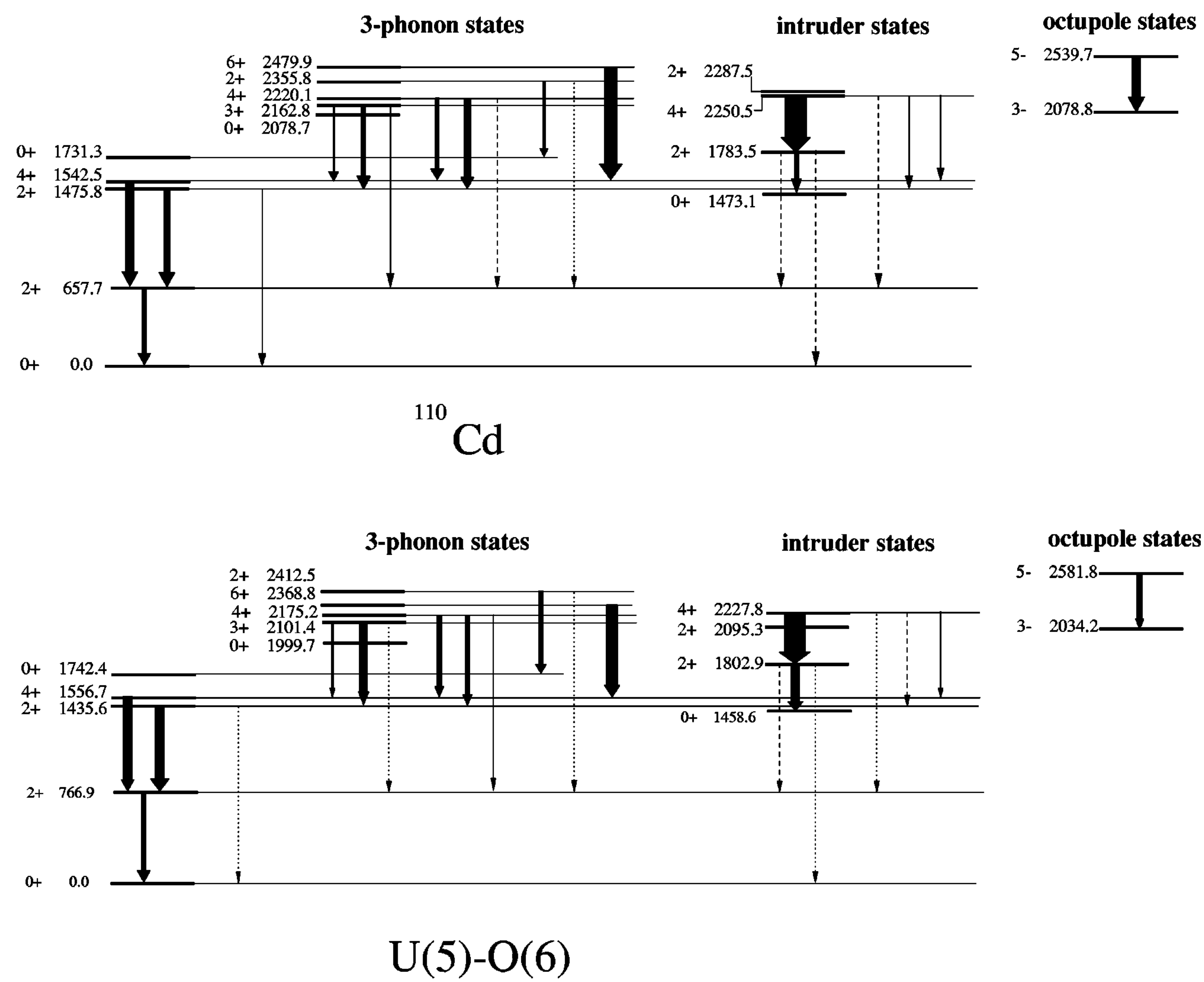


FIG. 7. Comparison between the experimental and theoretical level energies and $B(E2)$ values for the U(5)-O(6) model (see text). The widths of the arrows correspond to the magnitude of the experimental and theoretical $B(E2)$ values.

TABLE VII. Comparison of experimental and theoretical $B(E1)$ values for states in $^{110}$Cd.

| Transition | $E_\gamma$ [keV] | $B(E1)_{expt.}$ [mW.u.] | *spdf*-IBM-1 [mW.u.] |
|---|---|---|---|
| $3^-_{oct} \rightarrow 2^+_{1ph}$ | 1421.1 | 0.2(1) | 0.4 |
| $3^-_{oct} \rightarrow 2^+_{2ph}$ | 603.1 | 0.4(1) | 0.03 |
| $3^-_{oct} \rightarrow 2^+_{1,intr}$ | 295.6 | $0.8^{+4}_{-3}$ | 0.0002 |
| $5^-_{oct} \rightarrow 4^+_{2ph}$ | 997.2 | 2.6(2) | 0.7 |

of a low-lying mixed-symmetry state does not strongly affect the other states, one notices its presence in the overpredicted $B(M1;2^+_{intr} \rightarrow 2^+_{1ph})$ value. In this context it is worth noting that the predicted $B(M1;2^+_{ms} \rightarrow 2^+_{1ph})$ value equals $0.38\mu_n^2$, which is clearly not observed for any $2^+$ state, including the state at 2.355 MeV proposed as a possible candidate in Ref. [12]. This absence of a mixed-symmetry state, combined with the relatively small $B(M1)$ values observed in $^{112}$Cd [33], casts some doubt on the existence of a low-lying mixed-symmetry state in $^{112}$Cd. While the magnetic dipole decay of the $3^+$ and $2^+$ states are well described in the model, a strong underprediction of the decay of the two $4^+$ states is observed. A possible explanation could be that these states are partially mixed with a two-quasiparticle state, although the good agreement of their electric quadrupole decay with experiment seems to contradict this.

### B. Negative parity states

The OCTUPOLE code also describes the negative-parity states based on the octupole vibration, using the *spdf* IBM-1 Hamiltonian, described in detail in [34]. Adopting the parameters describing the negative-parity states obtained in [28] for $^{112}$Cd excellent results are obtained. The theoretical octupole vibration is calculated at 2034 keV and the $5^-$ member of the quadrupole-octupole coupled (QOC) states at 2581 keV. Besides the good agreement in excitation energy, the theory also nicely reproduces the observed collective quadrupole transition between these states (see Table IV), confirming the QOC character of the $5^-$ state at 2539.7 keV. Table VII compares the experimental $B(E1)$ values with the ones obtained with the *spdf* IBM-1 calculation using the transition operator described in [34]. In general the theoretical values are within the order of magnitude of the experimental values, except for the decay of the octupole state to the $2^+_{1,intr}$ which is greatly underestimated. While the low transition probability is easily understood from the theoretical point of view, the large experimental value seems to confirm the insensitivity of $B(E1)$ transitions to the nature of states in this mass region, as discussed by Garrett *et al.* [35].

## V. CONCLUSION

The primary goal of this work was to examine the character of the states in $^{110}$Cd in the region up to 3 MeV. Toward this end, the $(n,n'\gamma)$ reaction has been used to perform a set of measurements consisting of $\gamma$-ray excitation functions and angular distributions. The former allowed us to add ten new transitions and one new level to the level scheme of $^{110}$Cd. The latter permitted the extraction of lifetimes of 16 excited states, of which 12 were previously unknown, and the determination of the multipole-mixing ratios. At the same time, we were able to determine the $B(E2,2^+_{1,intr} \rightarrow 0^+_{intr})$ value. Unfortunately, the lifetime of the $0^+_{intr}$ state at 1473.1 keV was too long to be determined by this method. As expected, the transition $4^+_{intr} \rightarrow 2^+_{1,intr}$ is very collective. As discussed in Ref. [17], we see that the three-phonon states have transitions to the two-phonon states which are clearly collective.

Our data also permitted us to identify the $5^-$ member of the quadrupole-octupole coupled state via the collective electric quadrupole transition to the octupole state and to exclude the presence of a low-lying mixed symmetry state.

To study the intruder states, the data were compared to calculations using IBM-2 with configuration mixing and the U(5)-O(6) model. Both models yield good agreement with the experimental results with a slight preference for IBM-2. However, in view of the very reduced set of parameters and the use of dynamical symmetries in the U(5)-O(6) model, $^{110}$Cd should be considered as an excellent example of a nucleus described by this model. Therefore, this nucleus is not only a good vibrational nucleus but it also illustrates clearly the coexistence of two dynamical symmetries in a single nucleus and the influence of the common O(5) subgroup [31] needed to explain the $2^+_{3ph} \rightarrow 0^+_{2ph}$ decay [17]. This conclusion is not only of importance in the context of the U(5)-O(6) model [25], but more generally for particle-hole symmetries as discussed in Refs. [36–39].

## ACKNOWLEDGMENTS

This work was supported by the Swiss National Fund for Scientific Research and by the U.S. National Science Foundation under Grant No. PHY-9803784.

[1] G. Scharff-Goldhaber and J. Weneser, Phys. Rev. **98**, 212 (1955).
[2] A. Arima and F. Iachello, Ann. Phys. (N.Y.) **99**, 253 (1976).
[3] R. A. Meyer and L. Peker, Z. Phys. A **283**, 379 (1977).
[4] K. Heyde, P. Van Isaker, M. Waroquier, and G. Wenes, Phys. Rev. C **25**, 3160 (1982).
[5] J. Kern, A. Bruder, S. Drissi, V. A. Ionescu, and D. Kusnezov, Nucl. Phys. **A512**, 1 (1990).
[6] B. L. Cohen, R. Patell, A. Prakash, and E. J. Schneid, Phys. Rev. **135**, B383 (1964).
[7] N. Blasi, S. Micheletti, M. Pignanelli, R. De Leo, R. Hertenberger, M. Bisemberger, D. Hofer, H. Kader, P. Schiemenz, and G. Graw, Nucl. Phys. **A536**, 1 (1992).
[8] M. Pignanelli, N. Blasi, S. Micheletti, R. De Leo, M. A. Hofstee, J. M. Schippers, S. Y. van der Werf, and M. N. Harakeh, Nucl. Phys. **A519**, 567 (1990).

[9] J. Kumpulainen, R. Julin, J. Kantele, A. Passoja, W. H. Trzaska, E. Verho, J. Väärämäki, C. Cutoiu, and M. Ivascu, Phys. Rev. C **45**, 640 (1992).
[10] Y. Kawase, K. Okano, S. Uehara, and T. Hayashi, Nucl. Phys. **A193**, 204 (1972).
[11] L. L. Kiang, P. K. Teng, G. C. Kiang, W. S. Chang, and P. J. Tu, J. Phys. Soc. Jpn. **62**, 888 (1993).
[12] M. Bertschy, S. Drissi, P. E. Garrett, J. Jolie, J. Kern, S. J. Mannanal, J. P. Vorlet, N. Warr, and J. Suhonen, Phys. Rev. C **51**, 103 (1995); **52**, 1148 (1995).
[13] S. Yu. Araddad, A. M. Demidov, M. M. Dyufani, S. M. Zlitni, V. A. Kurkin, I. V. Mikhailov, D. M. Rateb, and S. M. Sergiwa, Yad. Fiz. **52**, 3 (1990) [Sov. J. Nucl. Phys. **52**, 1 (1990)].
[14] A. M. Demidov, S. M. Zlitni, V. A. Kurkin, J. M. Rateb, S. M. Sergiva, and A. M. Shermit, Bull. Rus. Acad. Sci. Phys. **56**, 8 (1992).
[15] M. Piiparinen *et al.*, Nucl. Phys. **A565**, 671 (1993).
[16] Yu. N. Lobach, A. D. Efimov, and A. A. Pasternak, Eur. Phys. J. A **6**, 131 (1999).
[17] F. Corminboeuf, T. B. Brown, L. Genilloud, C. D. Hannant, J. Jolie, J. Kern, N. Warr, and S. W. Yates, Phys. Rev. Lett. **84**, 4060 (2000).
[18] P. E. Garrett, N. Warr, and S. W. Yates, J. Res. Natl. Inst. Stand. Technol. **105**, 141 (2000).
[19] E. Sheldon and V. C. Rogers, Comput. Phys. Commun. **6**, 99 (1973).
[20] D. De Frenne, Nucl. Data Sheets **67**, 809 (1992).
[21] K. B. Winterbon, Nucl. Phys. **A246**, 293 (1975).
[22] T. Belgya, G. Molnär, and S. W. Yates, Nucl. Phys. **A607**, 43 (1996).
[23] D. G. Sarantites, N. R. Johnson, and H. W. Boyd, Nucl. Phys. **A138**, 115 (1969).
[24] J. L. Wood, K. Heyde, W. Nazarewiecz, M. Huyse, and P. Van Duppen, Phys. Rep. **215**, 101 (1992), and references therein.
[25] H. Lehmann and J. Jolie, Nucl. Phys. **A588**, 623 (1995).
[26] D. Kusnezov, computer code OCTUPOLE, 1987 (unpublished).
[27] K. Heyde, J. Jolie, J. Moreau, J. Ryckebusch, M. Waroquier, P. Van Duppen, M. Huyse, and J. L. Wood, Nucl. Phys. **A466**, 189 (1987).
[28] M. Délèze, S. Drissi, J. Kern, P. A. Tercier, J. P. Vorlet, J. Rikovska, T. Otsuka, S. Judge, and A. Williams, Nucl. Phys. **A551**, 269 (1993).
[29] H. Lehmann, P. E. Garrett, J. Jolie, C. A. McGrath, Minfang Yeh, and S. W. Yates, Phys. Lett. B **387**, 259 (1996).
[30] S. Drissi *et al.*, Nucl. Phys. **A614**, 137 (1997).
[31] J. Jolie and H. Lehmann, Phys. Lett. B **342**, 1 (1995).
[32] N. Warr, S. Drissi, P. E. Garrett, J. Jolie, J. Kern, H. Lehmann, S. J. Mannanal, and J.-P. Vorlet, Nucl. Phys. **A636**, 379 (1998).
[33] P. E. Garrett, H. Lehmann, C. A. McGrath, Minfang Yeh, and S. W. Yates, Phys. Rev. C **54**, 2259 (1996).
[34] H. Lehmann *et al.*, Phys. Rev. C **60**, 024308 (1999).
[35] P. E. Garrett, H. Lehmann, J. Jolie, C. A. McGrath, Minfang Yeh, and S. W. Yates, Phys. Rev. C **59**, 2455 (1999).
[36] C. De Coster, K. Heyde, B. Decroix, P. Van Isaker, J. Jolie, H. Lehmann, and J. L. Wood, Nucl. Phys. **A600**, 251 (1996).
[37] H. Lehmann, J. Jolie, C. De Coster, B. Decroix, K. Heyde, and J. L. Wood, Nucl. Phys. **A621**, 767 (1997).
[38] C. De Coster, B. Decroix, K. Heyde, J. L. Wood, J. Jolie, and H. Lehmann, Nucl. Phys. **A621**, 802 (1997).
[39] C. De Coster, B. Decroix, K. Heyde, J. Jolie, H. Lehmann, and J. L. Wood, Nucl. Phys. **A651**, 31 (1999).